The *ORMDL3* asthma susceptibility gene regulates systemic ceramide levels without altering key asthma features in mice

Nincy Debeuf, MSc[a,b], Assem Zhakupova, PhD[c], Regula Steiner, PhD[c], Sofie Van Gassen, PhD[d,e], Kim Deswarte, BSc[a,b], Farzaneh Fayazpour, PhD[b,f], Justine Van Moorleghem, BSc[a,b], Karl Vergote, BSc[a,b], Benjamin Pavie, MSc[g], Kelly Lemeire, MSc[h], Hamida Hammad, PhD[a,b], Thorsten Hornemann, PhD[c], Sophie Janssens, PhD[b,f*] and Bart N. Lambrecht, MD, PhD[a,b,i*].

a. Laboratory of Mucosal Immunology and Immunoregulation, VIB Center for Inflammation Research, Ghent, Belgium
b. Department of Internal Medicine and Pediatrics, Ghent University, Ghent, Belgium
c. Institute of Clinical Chemistry, University and University Hospital Zurich, Zurich, Switzerland
d. Data Mining and Modeling for Biomedicine, VIB Center for Inflammation Research, Ghent, Belgium
e. Department of Applied Mathematics, Computer Science and Statistics, Ghent University, Ghent, Belgium
f. Laboratory for ER Stress and Inflammation, VIB Center for Inflammation Research, Ghent, Belgium
g. VIB Bioimaging Core, VIB Center for Inflammation Research, Ghent, Belgium
h. VIB Center for Inflammation Research, Ghent, Belgium
i. Department of Pulmonary Medicine, Erasmus Medical Center, Rotterdam, The Netherlands.

*These authors contributed equally to this work.

Correspondence:
Bart N. Lambrecht, MD, PhD
VIB-UGent Center for Inflammation Research
Technologiepark- Zwijnaarde 71
9052 Zwijnaarde (Gent)
Belgium
Phone: +32-9-3313607
Fax: +32-9-2217673

Email: bart.lambrecht@ugent.be
ORCID 0000-0003-4376-6834

FUNDING

ND is supported by a Fonds Wetenschappelijk Onderzoek Vlaanderen (FWO) grant (11Y8417N). BNL is supported by an European Research Council (ERC)-advanced grant (ERC-ADG 789384), a Concerted Research Initiative Grant (GOA) of Ghent University, and an Excellence of Science (EOS) research grant (project 30565447). SJ is a recipient of an ERC Consolidator Grant (ERC-CoG 819314). BNL and SJ are holders of several FWO program grants, a UGent MRP grant (Group-ID) and a Stichting tegen Kanker Grant.

ABSTRACT

Background: Genome-wide association studies in asthma have repeatedly identified single nucleotide polymorphisms in the ORM (yeast)-like protein isoform 3 (*ORMDL3*) gene across different populations. Although the ORM-homologues in yeast are well-known inhibitors of sphingolipid (SL) synthesis, it is still unclear whether and how mammalian ORMDL3 regulates SL metabolism and whether altered SL synthesis would be causally related to asthma risk.

Objective: To examine the *in vivo* role of ORMDL3 in SL metabolism and allergic asthma

Methods: *Ormdl3*-LacZ reporter mice, gene deficient *Ormdl3*$^{-/-}$ and overexpressing *Ormdl3*$^{Tg/wt}$ mice were exposed to physiologically relevant aeroallergens such as house dust mite or *Alternaria alternata* to induce experimental asthma. Mass spectrometry based sphingolipidomics was performed, and airway eosinophilia, Th2 cytokine production, Ig synthesis, airway remodeling and bronchial hyperreactivity measured.

Results: HDM challenge significantly increased total sphingolipids in the lung of HDM-sensitized mice compared to controls. In *Ormdl3*$^{Tg/wt}$ mice, the allergen-induced increase in lung ceramides was significantly reduced, whereas total sphingolipid levels were not affected. Conversely, in liver and serum, total sphingolipids including ceramides were increased in *Ormdl3*$^{-/-}$ mice, while they were lowered in *Ormdl3*$^{Tg/wt}$ mice. This difference was independent of allergen exposure. Despite these changes, all features of asthma were identical between wildtype, *Ormdl3*$^{Tg/wt}$ and *Ormdl3*$^{-/-}$ mice, across several models of experimental asthma.

Conclusion: ORMDL3 regulates systemic ceramide levels, but genetically interfering with *Ormdl3* expression does not result in altered experimental asthma.

KEY MESSAGES

- *Ormdl3* expression levels did not affect allergic asthma development driven by house dust mite or *Alternaria alternata*.
- ORMDL3 negatively regulated ceramide levels, but this did not result in altered experimental asthma.

CAPSULE SUMMARY

ORMDL3 regulates systemic ceramide levels, but genetically interfering with *Ormdl3* expression does not result in altered experimental asthma.

KEY WORDS

Asthma, ORMDL3, house dust mite, *Alternaria alternata*, sphingolipids, ceramides

ABBREVIATIONS

ALT: *Alternaria alternata*
BAL: Bronchoalveolar lavage
BHR: Bronchial hyperreactivity
ER: Endoplasmic reticulum
GCM: Goblet cell metaplasia
GWAS: Genome-wide association study
HDM: House dust mite
Ig: Immunoglobulin
IL: Interleukin
MLN: Mediastinal lymph node
OVA: Ovalbumin
ORMDL3: ORM (yeast)-like protein isoform 3

α-SMA: alpha-smooth muscle actin

SNPs: Single nucleotide polymorphisms

SPT: Serine palmitoyl transferase

INTRODUCTION

Allergic asthma results from a complex gene-by-environment interaction and is currently still on the rise (1). Single nucleotide polymorphisms (SNPs) on chromosome 17q12-21 confer the most significant and replicated genetic susceptibility to childhood-onset asthma and rhinovirus-induced wheezing illness in childhood (2-8). Many of these SNPs fall within the promoter region of the ORM (yeast)-like protein isoform 3 (*ORMDL3*) gene and induce slightly elevated levels of *ORMDL3*, particularly in T lymphocytes and following stimulation of PBMCs with allergens (2,9-11). *Ormdl3* mRNA is also upregulated in murine asthma models, driven by ovalbumin (OVA), house dust mite (HDM) or *Alternaria alternata* (12,13). However, studies addressing the functional role of ORMDL3 in asthma generated conflicting conclusions. Both transgenic overexpression as well as genetic deficiency of *Ormdl3* can enhance key asthma features, whereas one study showed that *Ormdl3* deficiency suppressed only bronchial hyperreactivity (BHR) (14-16). Given the multitude of genetic association studies in humans, the currently prevailing hypothesis is still that ORMDL3 overexpression has a causal role in asthma development or progression.

The molecular mechanism by which ORMDL3 contributes to asthma is still a matter of intense debate (6,8). ORMDL3 is member of an evolutionary conserved family of endoplasmic reticulum (ER)-residing proteins, and has two paralogues in vertebrates, ORMDL1 and ORMDL2, that have not been associated with asthma (17). In yeast, the ORM homologues are described as regulators of *de novo* sphingolipid synthesis by controlling the activity of the rate limiting enzyme serine palmitoyl transferase (SPT) (18-23). In mammals however, ORMDLs lack the N-terminal phosphorylation site that is crucial for SPT regulation in yeast. Mammalian SPT activity seems to be affected only when all ORMDL paralogues are overexpressed or downregulated simultaneously (17,24-26), making it unlikely that SNPs in only *ORMDL3* influence asthma by SPT inhibition. As an ER-resident protein, ORMDL3 has

also been described to affect calcium metabolism and the unfolded protein response, influencing cytokine secretion by structural or immune cells (6,12,27-29). However, most molecular studies on ORMDL3 were performed *in vitro* and have led to contradictory results due to the use of different cell lines and distinct approaches to measure total sphingolipid *de novo* synthesis and to control *ORMDL3* expression. Furthermore, many studies were performed on epithelial cells, macrophages, mast cells and eosinophils (6,12,13,29-31), whereas it has been recently demonstrated that chr17q12-21 SNPs affect *ORMDL3* expression most prominently in T-cells (9).

Here, we addressed the role of ORMDL3 in SL metabolism and asthma in newly generated *Ormdl3*-LacZ reporter mice, full *Ormdl3* KO mice (*Ormdl3*$^{-/-}$), and mice overexpressing murine *Ormdl3* from a Bacterial Artificial Chromosome (BAC)-transgene (*Ormdl3*$^{Tg/wt}$). Using these unique gene-modified mice and their littermate controls, we found that ORMDL3 expression influences ceramide levels in serum and liver and to a lesser extent in lung tissue. At the same time, interfering with *Ormdl3* did not impact on key asthma parameters in various allergen driven asthma models. These data do not support the currently prevailing paradigm that *ORMDL3* drives asthma by interfering with SPT activity or sphingolipid homeostasis.

METHODS

Mice

Ormdl3-LacZ reporter mice were generated by inserting a targeting construct of the European Conditional Mouse Mutagenesis consortium (project 72180) into the first intron of the *Ormdl3* gene (Fig. 1A). This construct contains a sequence that consists of an En2 splice acceptor site, an internal ribosome entry site, a LacZ sequence, a polyA-tail, a loxP site, and a

148 neomycin coding sequence driven by a human β-actin promoter that is flanked by 2 Flp
149 recombinase target (FRT) sites. ORMDL3 knockout (*Ormdl3*$^{-/-}$) mice and ORMDL3
150 transgenic (*Ormdl3*$^{Tg/wt}$) mice were previously described (25). All mice were backcrossed for
151 at least 10 crosses onto a C57BL/6 background. 1-DER mice express an MHC class II–
152 restricted TCR specific for Der p 1 on their CD4 T cells and were generated as previously
153 described (32-34). Mice were bred under specific pathogen–free conditions at the animal
154 house of the VIB/UGhent Center for Inflammation Research. Experiments were carried out
155 using age- and gender-matched groups. All mice were used between 6-14 weeks of age. All
156 animal procedures were approved by the Ethical Committee of Ghent University.
157
158 **Models of allergic asthma**
159 The HDM-induced asthma model was performed as described before (35). In brief, mice were
160 sensitized intratracheally (i.t.) on day 0 with 1 μg HDM extract (Greer Laboratories, Lenoir,
161 USA) or saline, followed by 10 μg intranasal (i.n.) challenges from day 6 to 10. On day 14,
162 mice were euthanized by an overdose pentobarbital. In the chronic HDM-induced asthma
163 model, mice were instilled i.n. with 10 ug HDM, or saline as a control, three times a week for
164 5 weeks. Asthma features were determined 3 days after the last challenge. In the *Alternaria*-
165 induced asthma model, mice were instilled i.n. with 20ug *Alternaria alternata* (Greer
166 Laboratories) three times a week for 3 weeks. All i.t. and i.n. treatments were given in 80 and
167 40 ul PBS, respectively, and under light isoflurane anesthesia.
168 Bronchoalveolar lavage (BAL) was performed using 3x1ml of EDTA-containing PBS (0,5
169 mM). Blood was obtained from the iliac vein in non-coated Eppendorf tubes to prepare
170 serum. Single cells suspensions from mediastinal lymph nodes were obtained by
171 homogenizing the organ through a 100 um cell sieve. Cells were restimulated *ex vivo* with 15
172 ug/ml HDM for 3 days and supernatants were collected for ELISA (Ready-set-go kits from

eBioscience). The left lung was fixed overnight in 4% paraformaldehyde and was used for histology. Right lung tissue was snap frozen in liquid nitrogen and kept at -80°C until used for RNA extraction.

BHR determination

Mice were anesthetized with urethane, paralyzed with D-tubocurarine, tracheostomized, and intubated with a 20-G catheter, followed by mechanical ventilation in a Flexivent apparatus (SCIREQ). Respiratory frequency was set at 150 breaths/min with a tidal volume (Vt) of 10 ml/kg, and a positive-end expiratory pressure (PEEP) of 3 cm H_2O was applied. Increasing concentrations of methacholine were nebulized (0–400 mg/ml) for 12 seconds and dynamic resistance, elastance and compliance were recorded by 12 repeat measurements during 2 minutes per dose. Baseline resistance was restored in between the doses.

Histology

After overnight fixation in 4% paraformaldehyde solution, tissues were embedded in paraffin, cut into 5 um slices and stained with either Periodic Acid-Schiff (PAS) or processed for immunochemistry. Periodic Acid-Schiff staining was performed as described in Debeuf *et al*. (2016). To detect peribronchial α-smooth muscle actin (α-SMA), lung sections were overnight incubated with an anti-α-SMA primary antibody (A2547, Sigma-Aldrich). Species- and isotype-matched antibodies were used as negative controls. Immunoreactivity was detected by sequential incubations of lung sections with a biotinylated secondary Ab (E0433, Dako, Belgium), Vectastain Elite ABC kit (Vector Laboratories, Burlingame, California, USA), followed by 3,3-diaminobenzidine chromogen (Dako). Sections were mounted by use of Entellan mounting medium (Merck Millipore).

198 **Lipidomics**

199 Individual sphingolipid species were quantified by a novel LC-MS method for a
200 comprehensive analysis of typical and atypical sphingolipid species. A lipidomics profiling
201 was done in 20 µL mouse serum or 20 µg of homogenate from lung tissue were extracted
202 using the MMC protocol as described previously (36). d7-sphinganine, d7-sphingosine, Cer
203 d18:0/12:0, Cer d18:1/12:0, SM d18:1/12:0, GluCer d18:1/18:0 and d7-S1P were used as
204 internal standards. C18-column-based method for chromatographic separation and MS
205 analysis was used, as described previously (36).

206

207 **Statistical analyses**

208 For all experiments, normality of each group was first checked by Shapiro-Wilk statistical
209 test. If data sets were normally distributed, a One-Way ANOVA test was performed. In case
210 of not normally distributed data, a Kruskal-Wallis test was done. All statistical tests were
211 performed in GraphPad Prism.

212

213 **RESULTS**

214 **Effect of allergen challenge on ORMDL3 expression in asthma**

215 One of the major drawbacks in the ORMDL3 field is the lack of specific antibodies, due to
216 the large sequence homology with ORMDL1 and ORMDL2 (84% and 83%, respectively).
217 Many investigators have therefore relied on *ORMDL3* mRNA analysis of isolated tissues or
218 cells, without confirming where exactly ORMDL3 is expressed. To be able to better address
219 ORMDL3 expression, *Ormdl3*-LacZ reporter mice were generated by inserting a targeting
220 construct into the first intron of *Ormdl3* (Fig. 1A)(25). Although these mice still express some
221 basal *Ormdl3* (Fig. 1B), β-galactosidase activity can be used as readout for *Ormdl3* promoter
222 activation. We first compared ORMDL3 expression levels in different tissues in steady state

mice. Despite the fact that *ORMDL3* is an asthma susceptibility gene, β-galactosidase expression was relatively low in lung tissue, especially compared to liver, and white and brown adipose tissues where ORMDL3 was abundantly present (Fig. 1C and Suppl. Fig. 1A). Similar results were obtained by RT-qPCR (Fig. 1D), consistent with RNA-seq data derived from the Genevestigator database (Suppl. Fig. 1B)(37). Previous studies suggested that epithelial cells would be the main cell type expressing ORMDL3 in the lung (14). However, in our hands, immunohistochemistry revealed diffuse and low β-galactosidase activity in subepithelial and vascular smooth muscle cells, epithelial cells and fibroblasts (Fig. 1E). On the contrary, high β-galactosidase activity was seen in white adipose tissue (Fig. 1E), consistent with mRNA expression data.

To address whether ORMDL3 expression was induced by allergen challenge *in vivo*, we employed a previously established model in which inhaled HDM challenge of HDM-sensitized mice leads to airway eosinophilia (Fig. 1F) (35). No increase in lung β-galactosidase activity was seen in allergen-challenged mice compared to control PBS exposed mice (Fig. 1G and Suppl. Fig. 1C). These results showed that ORMDL3 expression in mouse lungs is low and did also not increase after allergen challenge using sensitized mice.

Characterization of *Ormdl3*$^{Tg/wt}$ and *Ormdl3*$^{-/-}$ mice

To assess the effects of altered ORMDL3 expression levels *in vivo*, we have recently generated *Ormdl3*-overexpressing mice (*Ormdl3*$^{Tg/wt}$) and gene deficient *Ormdl3*$^{-/-}$ mice (25). Before we used these mice in asthma experiments, we wanted to address if immune cell development was affected by a systemic change in *Ormdl3* expression. Mice from both strains were healthy and did not develop a spontaneous phenotype, even with ageing (data not shown). We stained cells with a broad panel of antibodies recognizing various lymphocytes and myeloid cells and used the FlowSOM automatic gating and visualization tool to assess the

immune cell landscape of *Ormdl3*$^{Tg/wt}$ and *Ormdl3*$^{-/-}$ mice in the most unbiased manner (38-40). Although there was a trend to an increased number of splenic cells in *Ormdl3*$^{Tg/wt}$ mice (Fig. 2A/B), none of the well known or less defined immune cell clusters were significantly altered compared with littermate controls (Fig. 2C/D). Likewise, FlowSOM trees represented a similar immune landscape between *Ormdl3*$^{-/-}$ mice and littermate controls (Fig. 2E-H). These data suggest that genetic alteration of ORMDL3 does not affect the immunome in a major manner.

Effect of altered ORMDL3 expression on sphingolipid concentration

In yeast, it has been conclusively demonstrated that ORM-proteins regulate *de novo* sphingolipid synthesis via controlling SPT activity. Therefore a dysregulation of sphingolipid *de novo* synthesis was proposed as a pathophysiological mechanism by which ORMDL3 promotes asthma (for a schematic overview of SL *de novo* synthesis, see Suppl. Fig. 2A) (8,18-23,41). We therefore assessed whether ORMDL3 affects sphingolipid metabolism in the context of allergic asthma by using our transgenic mice. Since there are three ORM paralogues expressed in mice, it was also important to assess if deficiency or overexpression of *Ormdl3* causes a compensatory change in *Ormdl1* or *Ormdl2* expression. For lung tissue, *Ormdl3* transcript levels were 6 fold increased in *Ormdl3*$^{Tg/wt}$ and expression levels were comparable for non-asthmatic (PBS/HDM group) and asthmatic (HDM/HDM group) conditions. A compensatory change in *Ormdl1* or *Ormdl2* expression was not observed (Fig. 3A). In *Ormdl3*$^{-/-}$ mice, transcript levels of *Ormdl3* were absent, without a sign of compensatory upregulation of *Ormdl1* or *Ormdl2* (Fig. 3B). Again, we did not observe any induction of *Ormdl3* mRNA upon asthmatic challenge (Fig. 3A-B).

Next, we investigated how asthma and ORMDL3 expression influenced the sphingolipid profile in various organs. We observed a mixed picture, depending on the analyzed tissue. In

lung, total sphingolipid levels were increased in asthmatic mice compared to non-asthmatic mice, confirming previous observations (13,42), but this increase was clearly independent of *Ormdl3* (Fig. 3C/D). In line with this, full sphingolipidomics analysis revealed an increase of ceramides in lungs of asthmatic mice (Fig. 3E/F), which appeared not affected by the absence of ORMDL3 (Fig. 3F). However, upon overexpression of ORMDL3, ceramide levels in the lung were slightly decreased, consistent with a role for ORMLD3 in blocking ceramide synthesis (13,43)(Fig. 3E). This was much more pronounced in the serum (Fig. 3G/H) and several other tissues, such as liver and fat in which ORMDL3 is higher expressed (Fig. 1C, Fig. 3G/H and Suppl. Fig. 2). These effects were not limited to ceramides but could also be observed for other sphingolipid species. For instance, sphingosine-1-phosphate (S1P) and sphinganine-1-phosphate (SA1P) were upregulated in serum from *Ormdl3*$^{-/-}$ mice and reduced in *Ormdl3*$^{Tg/wt}$ mice (Fig. 3C/D). A similar pattern was observed for hexosylceramides and sphingomyelins (Suppl. Fig. 2E-G). In summary, sphingolipid homeostasis seems to be mostly influenced in those tissues where ORMDL3 is abundantly expressed. For lung, we did not see a major influence of ORMDL3 expression on the asthma-induced change in the SL profile.

Genetic alteration of ORMDL3 expression levels does not affect key asthma parameters

Having found that genetic interference with the expression levels of ORMDL3 led to alterations in ceramide levels, we next addressed if key asthma parameters would be altered in *Ormdl3*$^{Tg/wt}$ or *Ormdl3*$^{-/-}$ mice, and experiments were each time compared to proper littermate wildtype controls. In HDM-sensitized, but not mock-sensitized, *Ormdl3*$^{wt/wt}$ mice, there was eosinophil, T cell and B cell infiltration in bronchoalveolar lavage (BAL) fluid, IL-5 and IL-13 cytokine production in the MLN, and HDM-specific IgE production in the serum, and bronchial hyperreactivity in response to increasing doses of metacholine (Fig. 4A-D and

298 Suppl. Fig. 3A/B). Strikingly, none of these key HDM-induced asthma parameters were
299 altered in *Ormdl3*$^{Tg/wt}$ mice. A previous study suggested the involvement of ORMDL3 in
300 airway remodeling, characterized by goblet cell metaplasia (GCM) and hypertrophia of α-
301 smooth muscle actin (α-SMA) expressing myofibroblasts (Miller et al. 2014). In *Ormdl3*$^{wt/wt}$
302 mice, HDM challenge of sensitized mice led to an increase in PAS-positive GCM, and of α-
303 SMA staining around the airways compared to non-sensitized mice (Fig. 4E-F), but again
304 these features were equally induced in *Ormdl3*$^{Tg/wt}$ mice. Even in a more chronic 5 week
305 model of HDM exposure, overexpression of ORMDL3 did not significantly influence cardinal
306 features of asthma (Suppl. Fig. 3C-G).
307 Recently, it has been shown that T-cells are the most prominent immune cells affected by
308 chr17q21 SNPs (9). Therefore, we wondered whether T-cell function would be intrinsically
309 affected by ORMDL3 overexpression. Although there were no obvious differences in the
310 outcome of the asthma experiments, it was still possible that T-cell function was slightly
311 affected, but that this only became apparent during competition experiments. Therefore, we
312 crossed *Ormdl3*$^{Tg/wt}$ with 1-DER mice, which contain T-cells that specifically react to the Der
313 p 1 peptide of HDM (32). *Ormdl3*$^{wt/wt}$ and *Ormdl3*$^{Tg/wt}$ 1-DER T cells were fluorescently
314 labelled and transferred into acceptor mice (Suppl. Fig. 4A), which were subsequently
315 exposed to HDM. Similar proportions of *Ormdl3*$^{wt/wt}$ and *Ormdl3*$^{Tg/wt}$ 1-DER T cells were
316 divided three days after transfer and numbers were equally high (Suppl. Fig. 4B-C). Thus, in
317 line with previous results, ORMDL3 did not affect HDM-specific proliferation by T cells
318 intrinsically.
319 To exclude allergen-dependent effects, *Ormdl3*$^{Tg/wt}$ mice were also exposed to a model driven
320 by the fungal extract *Alternaria alternata*. Mice were administered 20 μg *Alternaria* (ALT) or
321 PBS three times a week, for 3 weeks (Suppl. Fig. 5A). ALT-treated mice had elevated
322 expression levels of *Ormdl3* mRNA, confirming earlier findings (Miller et al. 2012) (Suppl.

Fig. 5B), however this could not be confirmed on protein level with *Ormdl3*-LacZ reporter mice (Suppl. Fig. 5C). In ALT exposed mice, there was a marked influx of eosinophils in the BAL fluid, an increase in ALT-specific IgE in the serum, Th2 cytokine production in the MLN, and development of BHR to methacholine compared with PBS exposed mice, but none of these features were altered in *Ormdl3*$^{Tg/wt}$ mice (Fig. 4G-I and Suppl. Fig. 5D-F).

It is most likely that the *ORMDL3* SNP at 17q12-21 that confers asthma risk leads to overexpression of ORMDL3, as has been demonstrated in T-cells (9). Since our transgenic mice overexpressing ORMDL3 did not have altered features of asthma, we also decided to perform all key asthma readouts in *Ormdl3*$^{-/-}$ mice in comparison with *Ormdl3*$^{+/+}$ littermates, again sensitizing mice to either HDM or ALT. Whereas all key features of allergic asthma like eosinophilia, Th2 cytokine production, HDM-specific serum IgE, BHR to methacholine, airway remodeling were induced by allergen challenge in *Ormdl3*$^{+/+}$ mice, none of these features were altered in *Ormdl3*$^{-/-}$ mice (Fig. 5A-F and Suppl. Fig. 6A). There was a small trend towards enhanced IL-17 production by allergen restimulated MLN T cells, but this was not accompanied by airway neutrophilia (Suppl. Fig. 6B). Similar conclusions were reached in the ALT model (Fig. 5G-I and Suppl. Fig. 6C-F). Therefore, neither ORMDL3 overexpression nor deletion affected key asthma parameters in various acute and chronic models driven by two different allergens.

DISCUSSION

During the last decade, genome-wide association studies have repeatedly and convincingly demonstrated that SNPs in the chr17q12-21 locus are associated with the early life onset of allergic asthma (2,3). Genotypes in the core region defined by the first genome-wide association study correlate with expression of 2 genes, *ORMDL3* and gasdermin B (*GSDMB*), making these prime candidate asthma genes, although recent studies have implicated gasdermin A (*GSDMA*) distal to and post-GPI attachment to proteins 3 (*PGAP3*) proximal to the core region as independent loci (8). There is much speculation on how ORMDL3 could regulate asthma. In yeast, ORM proteins control sphingolipid levels by regulating the enzyme SPT, the rate-limiting enzyme of *de novo* sphingolipid synthesis (18). A mouse study subsequently showed that interfering with SPT using the inhibitor myriocin reduced *de novo* sphingolipid synthesis and increased bronchial hyperreactivity (44). This led some to conclude that *ORMDL3* controls asthma via altered sphingolipid metabolism (41,45). However, despite extensive efforts, the molecular role of ORMDL3 in allergic asthma has not been unraveled yet.

Although the studies addressing the effect of inhibition of *de novo* SL synthesis using myriocin or genetic deficiency of SPT have yielded consistent results (13,24,26,44,46-50), the mouse studies investigating the role of ORMDL3 in asthma have been harder to reconcile. Miller *et al*. (2014) reported that C57BL/6 mice expressing high levels of human ORMDL3 developed stronger inflammation and BHR compared to wildtype mice in a mouse model driven by intraperitoneal immunization by OVA in alum followed by a series of OVA inhalation challenges (14). However, the same group also reported that BHR (but not inflammation) was increased in C57BL/6 mice lacking ORMDL3 specifically in epithelial cells (16), which makes the results hard to interpret. In contrary, Loser *et al*. (2016) reported that full *Ormdl3* gene deficient C57BL/6 mice were protected from developing BHR to

368 *Alternaria alternata*, whereas inflammation was only slightly affected. From these conflicting
369 studies, the conclusion would be that the role of ORMDL3 in experimental asthma is highly
370 contextual, and might be explained by subtle differences in animal models used by different
371 investigators, and whether the model employed overexpression of (human) *ORMDL3* or
372 genetic deficiency of endogenous mouse *Ormdl3*. To address this controversy regarding the
373 models used, we applied multiple models (acute versus chronic) and allergens (HDM,
374 *Alternaria*, and OVA, not shown) in newly generated *Ormdl3* BAC transgenic and *Ormdl3*$^{-/-}$
375 mice. We observed no differences in the severity of all key asthma parameters when *Ormdl3*
376 was either overexpressed or deleted from the mouse genome. At present, we can only
377 speculate about the differences between our negative results and the positive results reported
378 by others. One major difference is that others studying overexpression have employed the
379 human *ORMDL3* gene using a plasmid expression system or adenoviral overexpression of
380 murine *Ormdl3 in vivo*, which could have led to unphysiological levels of overexpression, or
381 overexpression in cell types that normally do not express ORMDL3. In addition, the reported
382 differences in *ORMDL3* expression based on the SNP genotype, is minor and significantly
383 smaller as it was reported for the transgenic mouse models. We have used a BAC transgenic
384 construct in which overexpression of *Ormdl3* is still driven by the endogenous *Ormdl3*
385 promotor. Modeling asthma in the mouse is difficult. It is possible that other environmental
386 triggers that often occur together with allergen exposure are necessary to unravel the link
387 between ORMDL3 and asthma, such as respiratory viruses or cigarette smoke. In fact, a
388 limitation of this study is the lack of a viral infection model, as recent epidemiological studies
389 suggest that SNPs in the chr17q12-21 locus combined with severe respiratory virus infections
390 do have a driving role in causing childhood-onset asthma (7,51,52). Interestingly, the same
391 SNPs also lead to protection from asthma upon microbial exposure (51), suggesting that this
392 locus is very environment-dependent and might be regulated by epigenetic modifications (53).

None of the studies addressing the relationship between ORMDL3 and asthma have so far studied experimental respiratory viral infections. Efforts are underway in our laboratory addressing the role of ORMDL3 in susceptibility to respiratory mouse pneumovirus infection and subsequent asthma development.

ORM-homologues in yeast are well-known inhibitors of *de novo* sphingolipid synthesis, whereas the role for the mammalian ORMDLs is still a matter of debate. We therefore examined sphingolipid synthesis by two approaches. First, we analyzed the total SL levels by quantifying the total C18-sphingoid base profile after chemical hydrolysis. If SPT-activity would be inhibited by ORMDL3, total sphingoid bases would be reduced in *Ormdl3*$^{Tg/wt}$ mice. However, neither in lungs of *Ormdl3*$^{Tg/wt}$ nor in *Ormdl3*$^{-/-}$ mice, a significant change in total sphingoid base levels could be detected. That corresponds to earlier reports that SPT-activity is not affected by changing ORMDL3 expression levels (25). Next, we performed sphingolipidomic analysis to quantify individual sphingolipid species, including ceramides, sphingomyelins, hexosyl ceramides and phosphorylated sphingoid bases (S1P, SA1P). In particular S1P has been extensively described to be involved in allergic asthma (54-58). Our results demonstrate an increase in serum S1P in *Ormdl3*$^{-/-}$ mice (Fig. 3D), which has also been seen in mice lacking ORMDL3 specifically in epithelial cells (16). Furthermore, *Ormdl3*$^{Tg/wt}$ mice had reduced levels of S1P (Fig. 3C), which is consistent with previous reports (43). However, the ORMDL3-dependent regulation of S1P did not result in an altered asthma phenotype.

Earlier reports have shown that ceramides are elevated in murine allergic asthma models and asthmatic patients and that inhibition of ceramide synthesis mitigates the allergic response (13,42). This was confirmed in our HDM model, which showed a significant increase in lung ceramides for asthmatic mice compared to non-asthmatic mice. This asthma dependent

increase in Cer was not influenced in *Ormdl3*$^{-/-}$ mice. On the other hand, it appeared to be hampered in *Ormdl3*$^{Tg/wt}$ mice. Of interest, serum ceramides were decreased in *Ormdl3*$^{Tg/wt}$ mice and conversely, were increased in *Ormdl3*$^{-/-}$ mice. Similar changes were seen in liver but not in BAT or WAT, which also express significant levels of ORMDL3 natively (Fig. 1C). A decrease in long-chain ceramides (C:24) has also been observed in mice overexpressing human ORMDL3 (43). Furthermore, Oyeniran et al. (2015) reported that all ceramide species were reduced upon overexpression of ORMDL3, provided that the degree of overexpression is moderate, which is the case in our *Ormdl3*$^{Tg/wt}$ mice. However, although serum (and lung) ceramide levels did change upon changing ORMDL3 expression levels, the allergic response was not affected, suggesting that the association of ORMDL3 with asthma would be hard to explain through alterations in ceramide levels.

In tissues where native ORMDL3 expression was the highest — based on the *Ormdl3*-LacZ reporter mouse — the effects on sphingolipid homeostasis were also the most pronounced. This may explain the moderate effects observed in lung. However, it is still unclear at which step ORMDL3 interferes in the sphingolipid synthesis pathway. In line with our previous data (25), we did not find a consistent change in total sphingolipid levels, which makes a direct effect of ORMDL3 on SPT activity questionable. Still, especially in liver but also other tissues, levels of several sphingolipid species were altered in mice with deregulated *Ormdl3*. Interestingly, the largest change was seen for serum SM, which is primarily formed in the liver and then secreted into blood in the form of lipoproteins. Among the different SL classes, we observed the most pronounced changes for Cer and SM whereas HexCer level were not much altered. This shows that mammalian ORMDL3 is somehow involved in the homeostasis of sphingolipids, but likely at a level downstream of SPT.

As an ER-residing protein, *in vitro* studies also reported a role for ORMDL3 in calcium homeostasis and the unfolded protein response (12,27,28), although there are also reports

demonstrating no role for ORMDL3 in the UPR (29). We measured UPR target gene expression in different tissues from *Ormdl3*$^{-/-}$ and *Ormdl3*$^{Tg/wt}$ mice, but could not find any differences compared to wildtype mice (data not shown), suggesting that the UPR was not affected upon changing ORMDL3 expression levels *in vivo*. It should be noted that a dramatic overexpression of ER proteins will affect ER homeostasis anyway, so the positive findings described *in vitro* may not be directly linked to ORMDL3.

Thus, in this study we found no causal relationship between ORMDL3 expression levels and severity of key asthma features in a HDM or *Alternaria*-driven allergic asthma model, despite clear alterations in sphingolipid levels in mice overexpressing or lacking ORMDL3. We therefore do not support the hypothesis that ORMDL3 controls asthma by altering sphingolipid metabolism. More research is needed on the causal relationship between respiratory virus infection, SNPs at 17q21, ORMDL3 levels and asthma risk, before we can definitively exclude a major role for ORMDL3 in asthma.

ACKNOWLEDGEMENTS

We thank all technicians of the Lambrecht-Hammad lab for their technical support, in particular Manon Vanheerswynghels, Sofie De Prijck and Caroline De Wolf.

REFERENCES

1. ***Lambrecht BN, Hammad H. The immunology of the allergy epidemic and the hygiene hypothesis. Nat Immunol. Nature Publishing Group; 2017 Sep 19;18(10):1076–83.***

2. ***Moffatt MF, Kabesch M, Liang L, Dixon AL, Strachan D, Heath S, et al. Genetic variants regulating ORMDL3 expression contribute to the risk of childhood asthma. Nature. Nature Publishing Group; 2007 Jul 26;448(7152):470–3.***

3. ***Zhao Y-F, Luo Y-M, Xiong W, Wu X-L. Genetic variation in ORMDL3 gene may contribute to the risk of asthma: a meta-analysis. Hum Immunol. 2014 Sep;75(9):960–7.***

4. *Bouzigon E, Corda E, Aschard H, Dizier M-H, Boland A, Bousquet J, et al. Effect of 17q21 variants and smoking exposure in early-onset asthma. N Engl J Med. 2008 Nov 6;359(19):1985–94.*

5. *Andiappan AK, Sio YY, Lee B, Suri BK, Matta SA, Lum J, et al. Functional variants of 17q12-21 are associated with allergic asthma but not allergic rhinitis. J Allergy Clin Immunol. 2016 Mar;137(3):758–66.e3.*

6. *Zhang Y, Willis-Owen SAG, Spiegel S, Lloyd CM, Moffatt MF, Cookson WOCM. The ORMDL3 Asthma Gene Regulates ICAM1 and has Multiple Effects on Cellular Inflammation. Am J Respir Crit Care Med. 2018 Oct 19;:rccm.201803–0438OC.*

7. *Calışkan M, Bochkov YA, Kreiner-Møller E, Bønnelykke K, Stein MM, Du G, et al. Rhinovirus wheezing illness and genetic risk of childhood-onset asthma. N Engl J Med. Massachusetts Medical Society; 2013 Apr 11;368(15):1398–407.*

8. *Stein MM, Thompson EE, Schoettler N, Helling BA, Magnaye KM, Stanhope C, et al. A decade of research on the 17q12-21 asthma locus: Piecing together the puzzle. J Allergy Clin Immunol. 2018 Sep;142(3):749–764.e3.*

9. *Schmiedel BJ, Seumois G, Samaniego-Castruita D, Cayford J, Schulten V, Chavez L, et al. 17q21 asthma-risk variants switch CTCF binding and regulate IL-2 production by T cells. Nat Commun. Nature Publishing Group; 2016 Nov 16;7(1):470.*

10. *Lluis A, Schedel M, Liu J, Illi S, Depner M, Mutius von E, et al. Asthma-associated polymorphisms in 17q21 influence cord blood ORMDL3 and GSDMA gene expression and IL-17 secretion. J Allergy Clin Immunol. 2011 Jun;127(6):1587–94.e6.*

11. *Schedel M, Michel S, Gaertner VD, Toncheva AA, Depner M, Binia A, et al. Polymorphisms related to ORMDL3 are associated with asthma susceptibility, alterations in transcriptional regulation of ORMDL3, and changes in TH2 cytokine levels. J Allergy Clin Immunol. 2015 Oct;136(4):893–903.e14.*

12. *Miller M, Tam AB, Cho JY, Doherty TA, Pham A, Khorram N, et al. ORMDL3 is an inducible lung epithelial gene regulating metalloproteases, chemokines, OAS, and ATF6. Proc Natl Acad Sci USA. 2012 Oct 9;109(41):16648–53.*

13. *Oyeniran C, Sturgill JL, Hait NC, Huang W-C, Avni D, Maceyka M, et al. Aberrant ORM (yeast)-like protein isoform 3 (ORMDL3) expression dysregulates ceramide homeostasis in cells and ceramide exacerbates allergic asthma in mice. J Allergy Clin Immunol. 2015 Oct;136(4):1035–6.*

14. *Miller M, Rosenthal P, Beppu A, Mueller JL, Hoffman HM, Tam AB, et al. ORMDL3 transgenic mice have increased airway remodeling and airway responsiveness characteristic of asthma. J Immunol. American Association of Immunologists; 2014 Apr 15;192(8):3475–87.*

15. *Löser S, Gregory LG, Zhang Y, Schaefer K, Walker SA, Buckley J, et al.*

Pulmonary ORMDL3 is critical for induction of Alternaria-induced allergic airways disease. J Allergy Clin Immunol. 2017 May;139(5):1496–1507.e3.

16. *Miller M, Tam AB, Mueller JL, Rosenthal P, Beppu A, Gordillo R, et al. Cutting Edge: Targeting Epithelial ORMDL3 Increases, Rather than Reduces, Airway Responsiveness and Is Associated with Increased Sphingosine-1-Phosphate. J Immunol. American Association of Immunologists; 2017 Apr 15;198(8):3017–22.*

17. *Hjelmqvist L, Tuson M, Marfany G, Herrero E, Balcells S, Gonzàlez-Duarte R. ORMDL proteins are a conserved new family of endoplasmic reticulum membrane proteins. Genome Biol. BioMed Central; 2002;3(6):RESEARCH0027.*

18. *Breslow DK, Collins SR, Bodenmiller B, Aebersold R, Simons K, Shevchenko A, et al. Orm family proteins mediate sphingolipid homeostasis. Nature. Nature Publishing Group; 2010 Feb 25;463(7284):1048–53.*

19. *Han S, Lone MA, Schneiter R, Chang A. Orm1 and Orm2 are conserved endoplasmic reticulum membrane proteins regulating lipid homeostasis and protein quality control. Proceedings of the National Academy of Sciences. 2010 Mar 30;107(13):5851–6.*

20. *Sun Y, Miao Y, Yamane Y, Zhang C, Shokat KM, Takematsu H, et al. Orm protein phosphoregulation mediates transient sphingolipid biosynthesis response to heat stress via the Pkh-Ypk and Cdc55-PP2A pathways. Riezman H, editor. Mol Biol Cell. 2012 Jun;23(12):2388–98.*

21. *Walther TC. Keeping sphingolipid levels nORMal. Proc Natl Acad Sci USA. 2010 Mar 30;107(13):5701–2.*

22. *Shimobayashi M, Oppliger W, Moes S, Jenö P, Hall MN. TORC1-regulated protein kinase Npr1 phosphorylates Orm to stimulate complex sphingolipid synthesis. Riezman H, editor. Mol Biol Cell. 2013 Mar;24(6):870–81.*

23. *Roelants FM, Breslow DK, Muir A, Weissman JS, Thorner J. Protein kinase Ypk1 phosphorylates regulatory proteins Orm1 and Orm2 to control sphingolipid homeostasis in Saccharomyces cerevisiae. Proceedings of the National Academy of Sciences. 2011 Nov 29;108(48):19222–7.*

24. *Kiefer K, Carreras-Sureda A, García-López R, Rubio-Moscardó F, Casas J, Fabriàs G, et al. Coordinated regulation of the orosomucoid-like gene family expression controls de novo ceramide synthesis in mammalian cells. J Biol Chem. American Society for Biochemistry and Molecular Biology; 2015 Jan 30;290(5):2822–30.*

25. *Zhakupova A, Debeuf N, Krols M, Toussaint W, Vanhoutte L, Alecu I, et al. ORMDL3 expression levels have no influence on the activity of serine palmitoyltransferase. FASEB J. Federation of American Societies for Experimental BiologyBethesda, MD, USA; 2016 Dec;30(12):4289–300.*

26. *Siow DL, Wattenberg BW. Mammalian ORMDL Proteins Mediate the Feedback*

Response in Ceramide Biosynthesis. J Biol Chem. 2012 Nov 23;287(48):40198–204.

27. *Cantero-Recasens G, Fandos C, Rubio-Moscardó F, Valverde MA, Vicente R. The asthma-associated ORMDL3 gene product regulates endoplasmic reticulum-mediated calcium signaling and cellular stress. Hum Mol Genet. 2010 Jan 1;19(1):111–21.*

28. *Carreras-Sureda A, Cantero-Recasens G, Rubio-Moscardó F, Kiefer K, Peinelt C, Niemeyer BA, et al. ORMDL3 modulates store-operated calcium entry and lymphocyte activation. Hum Mol Genet. 2013 Feb 1;22(3):519–30.*

29. *Hsu KJ, Turvey SE. Functional analysis of the impact of ORMDL3 expression on inflammation and activation of the unfolded protein response in human airway epithelial cells. Allergy Asthma Clin Immunol. BioMed Central; 2013 Feb 1;9(1):4.*

30. *Bugajev V, Halova I, Draberova L, Bambouskova M, Potuckova L, Draberova H, et al. Negative regulatory roles of ORMDL3 in the FcεRI-triggered expression of proinflammatory mediators and chemotactic response in murine mast cells. Cellular and Molecular Life Sciences. Springer International Publishing; 2015 Sep 25;73(6):1265–85.*

31. *Ha SG, Ge XN, Bahaie NS, Kang BN, Rao A, Rao SP, et al. ORMDL3 promotes eosinophil trafficking and activation via regulation of integrins and CD48. Nat Commun. Nature Publishing Group; 2013;4(1):2479.*

32. *Dullaers M, Schuijs MJ, Willart M, Fierens K, van Moorleghem J, Hammad H, et al. House dust mite-driven asthma and allergen-specific T cells depend on B cells when the amount of inhaled allergen is limiting. J Allergy Clin Immunol. 2017 Jul;140(1):76–7.*

33. *Schuijs MJ, Willart MA, Vergote K, Gras D, Deswarte K, Ege MJ, et al. Farm dust and endotoxin protect against allergy through A20 induction in lung epithelial cells. Science. 2015 Sep 4;349(6252):1106–10.*

34. *Vanheerswynghels M, Toussaint W, Schuijs M, Vanhoutte L, Killeen N, Hammad H, et al. The Generation and Use of Allergen-Specific TCR Transgenic Animals. Methods Mol Biol. New York, NY: Springer New York; 2018;1799(2):183–210.*

35. *Debeuf N, Haspeslagh E, van Helden M, Hammad H, Lambrecht BN. Mouse Models of Asthma. Curr Protoc Mouse Biol. Hoboken, NJ, USA: John Wiley & Sons, Inc; 2016 Jun 1;6(2):169–84.*

36. *Atkinson D, Nikodinovic Glumac J, Asselbergh B, Ermanoska B, Blocquel D, Steiner R, et al. Sphingosine 1-phosphate lyase deficiency causes Charcot-Marie-Tooth neuropathy. Neurology. 2017 Feb 6;88(6):533–42.*

37. *Hruz T, Laule O, Szabo G, Wessendorp F, Bleuler S, Oertle L, et al. Genevestigator v3: a reference expression database for the meta-analysis of transcriptomes. Adv Bioinformatics. Hindawi; 2008;2008:420747–5.*

38. *Van Gassen S, Callebaut B, Van Helden MJ, Lambrecht BN, Demeester P, Dhaene T, et al. FlowSOM: Using self-organizing maps for visualization and interpretation of cytometry data. Brinkman RR, Aghaeepour N, Finak G, Gottardo R, Mosmann T, Scheuermann RH, editors. Cytometry A. Wiley-Blackwell; 2015 Jul;87(7):636–45.*

39. *Guilliams M, Dutertre C-A, Scott CL, McGovern N, Sichien D, Chakarov S, et al. Unsupervised High-Dimensional Analysis Aligns Dendritic Cells across Tissues and Species. Immunity. 2016 Sep 20;45(3):669–84.*

40. *Saeys Y, Van Gassen S, Lambrecht BN. Computational flow cytometry: helping to make sense of high-dimensional immunology data. Nat Rev Immunol. Nature Publishing Group; 2016 Jul;16(7):449–62.*

41. *Levy BD. Sphingolipids and susceptibility to asthma. Phimister EG, editor. N Engl J Med. 2013 Sep 5;369(10):976–8.*

42. *Masini E, Giannini L, Nistri S, Cinci L, Mastroianni R, Xu W, et al. Ceramide: a key signaling molecule in a Guinea pig model of allergic asthmatic response and airway inflammation. J Pharmacol Exp Ther. American Society for Pharmacology and Experimental Therapeutics; 2008 Feb;324(2):548–57.*

43. *Miller M, Rosenthal P, Beppu A, Gordillo R, Broide DH. Oroscomucoid like protein 3 (ORMDL3) transgenic mice have reduced levels of sphingolipids including sphingosine-1-phosphate and ceramide. J Allergy Clin Immunol. 2017 Apr;139(4):1373–4.*

44. *Worgall TS, Veerappan A, Sung B, Kim BI, Weiner E, Bholah R, et al. Impaired sphingolipid synthesis in the respiratory tract induces airway hyperreactivity. Sci Transl Med. 2013 May 22;5(186):186ra67–7.*

45. *Worgall TS. Sphingolipids, ORMDL3 and asthma: what is the evidence? Curr Opin Clin Nutr Metab Care. 2017 Mar;20(2):99–103.*

46. *Miyake Y, Kozutsumi Y, Nakamura S, Fujita T, Kawasaki T. Serine palmitoyltransferase is the primary target of a sphingosine-like immunosuppressant, ISP-1/myriocin. Biochemical and Biophysical Research Communications. 1995 Jun 15;211(2):396–403.*

47. *Hojjati MR, Li Z, Jiang X-C. Serine palmitoyl-CoA transferase (SPT) deficiency and sphingolipid levels in mice. Biochim Biophys Acta. 2005 Oct 15;1737(1):44–51.*

48. *Li Z, Park T-S, Li Y, Pan X, Iqbal J, Lu D, et al. Serine palmitoyltransferase (SPT) deficient mice absorb less cholesterol. Biochim Biophys Acta. 2009 Apr;1791(4):297–306.*

49. *Chakraborty M, Lou C, Huan C, Kuo M-S, Park T-S, Cao G, et al. Myeloid cell-specific serine palmitoyltransferase subunit 2 haploinsufficiency reduces murine atherosclerosis. J Clin Invest. American Society for Clinical Investigation; 2013 Apr;123(4):1784–97.*

631 ***50.*** ***Strettoi E, Gargini C, Novelli E, Sala G, Piano I, Gasco P, et al. Inhibition of***
632 ***ceramide biosynthesis preserves photoreceptor structure and function in a***
633 ***mouse model of retinitis pigmentosa. Proc Natl Acad Sci USA. 2010 Oct***
634 ***26;107(43):18706–11.***

635 ***51.*** ***Loss GJ, Depner M, Hose AJ, Genuneit J, Karvonen AM, Hyvärinen A, et al. The***
636 ***Early Development of Wheeze. Environmental Determinants and Genetic***
637 ***Susceptibility at 17q21. Am J Respir Crit Care Med. American Thoracic Society;***
638 ***2016 Apr 15;193(8):889–97.***

639 ***52.*** ***Wang X-H, Shu J, Jiang C-M, Zhuang L-L, Yang W-X, Zhang H-W, et al.***
640 ***Mechanisms and roles by which IRF-3 mediates the regulation of ORMDL3***
641 ***transcription in respiratory syncytial virus infection. Int J Biochem Cell Biol.***
642 ***2017 Jun;87:8–17.***

643 ***53.*** ***Kothari PH, Qiu W, Croteau-Chonka DC, Martinez FD, Liu AH, Lemanske RF, et***
644 ***al. Role of local CpG DNA methylation in mediating the 17q21 asthma***
645 ***susceptibility gasdermin B (GSDMB)/ORMDL sphingolipid biosynthesis***
646 ***regulator 3 (ORMDL3) expression quantitative trait locus. J Allergy Clin***
647 ***Immunol. 2018 Jun;141(6):2282–6.***

648 ***54.*** ***Jolly PS, Rosenfeldt HM, Milstien S, Spiegel S. The roles of sphingosine-1-***
649 ***phosphate in asthma. Mol Immunol. 2002 Sep;38(16-18):1239–45.***

650 ***55.*** ***Kleinjan A, van Nimwegen M, Leman K, Hoogsteden HC, Lambrecht BN. Topical***
651 ***treatment targeting sphingosine-1-phosphate and sphingosine lyase***
652 ***abrogates experimental allergic rhinitis in a murine model. Allergy. 2013***
653 ***Feb;68(2):204–12.***

654 ***56.*** ***Price MM, Oskeritzian CA, Falanga YT, Harikumar KB, Allegood JC, Alvarez SE,***
655 ***et al. A specific sphingosine kinase 1 inhibitor attenuates airway***
656 ***hyperresponsiveness and inflammation in a mast cell–dependent murine***
657 ***model of allergic asthma. Journal of Allergy and Clinical Immunology. 2013***
658 ***Feb;131(2):501–1.***

659 ***57.*** ***Karmouty-Quintana H, Siddiqui S, Hassan M, Tsuchiya K, Risse P-A, Xicota-Vila***
660 ***L, et al. Treatment with a sphingosine-1-phosphate analog inhibits airway***
661 ***remodeling following repeated allergen exposure. Am J Physiol Lung Cell Mol***
662 ***Physiol. 2012 Apr 15;302(8):L736–45.***

663 ***58.*** ***Oskeritzian CA, Hait NC, Wedman P, Chumanevich A, Kolawole EM, Price MM,***
664 ***et al. The sphingosine-1-phosphate/sphingosine-1-phosphate receptor 2 axis***
665 ***regulates early airway T-cell infiltration in murine mast cell-dependent acute***
666 ***allergic responses. J Allergy Clin Immunol. 2015 Apr;135(4):1008–18.e1.***

667

668 **FIGURE LEGENDS**

669 **Figure 1: *Ormdl3*-LacZ reportermice as a useful tool to study ORMDL3 expression**

A) *Ormdl3*-LacZ reportermice (*Ormdl3*$^{LacZ/LacZ}$) were generated by inserting a targeting construct of the EUCOMM consortium into the first intron of *Ormdl3*. Exon 2, exon 3 and part of exon 4 are flanked by two loxP sites, which enable the generation of conditional knockout mice upon crossing with mice expressing Cre-recombinase.
B) *Ormdl3* mRNA expression levels in lungs from *Ormdl3*$^{+/+}$, *Ormdl3*$^{LacZ/LacZ}$ and *Ormdl3*$^{-/-}$ mice. Expression values are shown relative to means of the wildtype group. Data were pooled from 2 experiments (n=7,6,4; means +/- SEM).
C) Western blot showing β-galactosidase expression in liver, lung, brown adipose tissue (BAT) and white adipose tissue (WAT) in three individual *Ormdl3*-LacZ reportermice. β-tubulin was used as a loading control.
D) *Ormdl3* transcript levels in lung, BAT, WAT and liver in wildtype mice. Expression values are shown relative to means of lung samples (means +/- SEM).
E) Immunohistochemistry analysis of β-galactosidase expression (blue) on lung OCT-inflated cryosections and WAT of *Ormdl3*-LacZ reportermice. Periodic-acid Schiff staining was used as counterstaining. A = airway; Bv = blood vessel; Alv = alveoli.
F) Scheme representing the acute house dust mite (HDM)-dependent asthma model.
G) Western blot showing β-galactosidase expression in lung tissue from mock- and HDM-challenged *Ormdl3*-LacZ reportermice.

Figure 2: Unbiased analysis of the immune landscape of *Ormdl3*$^{Tg/wt}$ and *Ormdl3*$^{-/-}$ mice
A) Splenic cell number from 6w old *Ormdl3*$^{wt/wt}$ and *Ormdl3*$^{Tg/wt}$ mice (n=5,5).
B/C) Numbers (B) and percentages (C) of different immune cell types in spleens from *Ormdl3*$^{wt/wt}$ and *Ormdl3*$^{Tg/wt}$ mice (n=5,5).
D) FlowSOM trees representing the splenic immune landscape in *Ormdl3*$^{wt/wt}$ and *Ormdl3*$^{Tg/wt}$ mice.
E) Splenic cell number from 6w old *Ormdl3*$^{+/+}$ and *Ormdl3*$^{-/-}$ mice (n=5,5).
F/G) Numbers (F) and percentages (G) of different immune cell types in spleens from *Ormdl3*$^{+/+}$ and *Ormdl3*$^{-/-}$ mice (n=5,5).
H) FlowSOM trees representing the splenic immune landscape in *Ormdl3*$^{+/+}$ and *Ormdl3*$^{-/-}$ mice.
Data information: All data were analysed with a Shapiro-Wilk normality test to assess whether the data was normally distributed. Parametric data were analysed with a t-test, whereas non-parametric data were analysed with a Mann-Whitney test. Data are shown as means +/- SEM. *$p<0.05$.

Figure 3: Effect of altered ORMDL3 expression on sphingolipid concentration
A/B) *Ormdl* mRNA expression levels in lung tissue from *Ormdl3*$^{wt/wt}$ and *Ormdl3*$^{Tg/wt}$ mice (A) or *Ormdl3*$^{+/+}$ and *Ormdl3*$^{-/-}$ mice (B) sensitized with saline (PBS) or house dust mite (HDM) and challenged with HDM. Expression values are shown relative to means of the mock-sensitized wildtype group (A: n=5,10,7,15; B: 8,8,3,6).
C/E) C18-sphingoid base levels in lung tissue from (non)-asthmatic *Ormdl3*$^{wt/wt}$ and *Ormdl3*$^{Tg/wt}$ mice (C) or *Ormdl3*$^{+/+}$ and *Ormdl3*$^{-/-}$ mice (E). Total SLs were extracted, and sphingosine (C18SO, grey) and sphinganine (C18SA, black) levels were analyzed after acid-base hydrolysis by liquid chromatography-mass spectrometry (C: n=8,13,6,10; E: n=5,5,7,7).
D/F) Sphingosine-1-phosphate (S1P, grey) and sphinganine-1-phosphate (SA1P, black) levels in serum from (non)-asthmatic *Ormdl3*$^{wt/wt}$ and *Ormdl3*$^{Tg/wt}$ mice (D) or *Ormdl3*$^{+/+}$ and *Ormdl3*$^{-/-}$ mice (F) (D: n=8,13,6,10; F: n=7,7,6,7).
G-J) Ceramide levels in lung tissue (G/H) or serum (I/J) from (non)-asthmatic *Ormdl3*$^{wt/wt}$ and *Ormdl3*$^{Tg/wt}$ mice (G/I) or *Ormdl3*$^{+/+}$ and *Ormdl3*$^{-/-}$ mice (H/J) (G/I: n=8,13,6,10; H: n=5,5,7,7; J:7,7,6,7).

C/D/G/I) Data were pooled from 3 independent experiments.
Data information: All data were analysed with a Shapiro-Wilk normality test to assess whether the data was normally distributed. Parametric data were analysed with an ordinary one-way ANOVA test with multiple comparison correction. Non-parametric data were analysed with an unpaired Kruskal-Wallis test with multiple correction. Data are shown as means +/- SEM. *p<0.05; **p<0.01, ***p<0.001, ****<0.0001.

Figure 4: ORMDL3 overexpression does not affect allergic asthma driven by HDM or *Alternaria alternata*

A) Eosinophil number in BAL fluid from (non)-asthmatic *Ormdl3*$^{wt/wt}$ and *Ormdl3*$^{Tg/wt}$ mice (n=5,11,7,14).
B) Protein levels of IL-5 and IL-13 secreted by MLN cells during restimulation with HDM (n=5,11,7,14).
C) Serum HDM-specific IgE levels (OD value) (n=4,11,6,13).
A-C) Data were pooled from 2 independent experiments.
D) Bronchial hyperreactivity upon exposure to increasing doses of methacholine (Mch) as measured with flexiVent (n=4,4,6,8).
E) Representative images of lung sections stained with either Periodic Acid-Schiff (PAS) or anti-α-smooth muscle actin (α-SMA) antibody. Scale bar = 100 um.
F) Quantification of PAS+ area and peribronchial α-SMA in lung tissue. Data were pooled from 3 independent experiments (n=1,15,1,9).
G) Eosinophil number in BAL fluid upon exposure to PBS or *Alternaria* (n=1,8,1,9).
H) Serum *Alternaria*-specific IgE levels (OD value) (n=1,6,1,4).
I) Bronchial hyperreactivity upon exposure to increasing doses of methacholine (Mch) as measured with flexiVent (SCIREQ) (n=1,7,1,4).
Data information: All data were analysed with a Shapiro-Wilk normality test to assess whether the data was normally distributed. Parametric data were analysed with an ordinary one-way ANOVA test with multiple comparison correction. Non-parametric data were analysed with an unpaired Kruskal-Wallis test with multiple correction. For F-I, a Mann-Whitney statistical test was performed between the HDM-sensitized groups. Data are shown as means +/- SEM. *p<0.05; **p<0.01, ***p<0.001.

Figure 5: Loss of *Ormdl3* expression does not affect allergic asthma driven by HDM or *Alternaria alternata*

A) Number of eosinophils in BAL fluid from (non)-asthmatic *Ormdl3*$^{+/+}$ and *Ormdl3*$^{-/-}$ mice (n=10,11,7,14).
B) Protein levels of IL-5 and IL-13 secreted by MLN cells during restimulation with HDM (n=10,11,7,14).
C) Serum HDM-specific IgG1, HDM-IgE and total IgE levels (OD value) (n=8,12,12,16).
A-C) Data were pooled from 2 experiments.
D) Bronchial hyperreactivity upon exposure to increasing doses of methacholine (Mch) as measured with flexiVent (n=4,4,6,6).
E) Representative images of lung sections stained with either Periodic Acid-Schiff (PAS) or anti-α-SMA antibody. Scale bar = 100um.
F) Quantification of PAS+ area (n=5,7,7,8) and peribronchial α-SMA (n=5,6,7,8) in lung tissue.
G) Number of eosinophils in BAL fluid from *Ormdl3*$^{+/+}$ and *Ormdl3*$^{-/-}$ mice exposed to PBS or *Alternaria* (n=2,10,2,9).
H) Serum *Alternaria*-specific IgE levels (OD value) (n=4,6,4,6).
I) Bronchial hyperreactivity upon exposure to increasing doses of methacholine (Mch) as

770 measured with flexiVent (SCIREQ) (n=4,6,4,6).
771 Data information: All data were analysed with a Shapiro-Wilk normality test to assess
772 whether the data was normally distributed. Parametric data were analysed with an ordinary
773 one-way ANOVA test with multiple comparison correction. Non-parametric data were
774 analysed with an unpaired Kruskal-Wallis test with multiple correction. Data are shown as
775 means +/- SEM. *p<0.05; **p<0.01, ***p<0.001, ****<0.0001.

SUPPLEMENTARY METHODS

Immunoglobulin production

Mice were bled under terminal anesthesia, and serum was collected by centrifugal phase separation to determine IgE and IgG1 levels by ELISA (BD Biosciences). For HDM-specific IgG1, ELISA plates were coated with 100 ug/ml HDM (Greer Laboratories). For HDM-specific IgE, ELISA plates were coated with an anti-IgE capture antibody (BD Biosciences) and the detection was performed with biotin-labeled HDM (100 ug/ml), diluted in PBS + 10% FCS.

Flow cytometry

Bronchoalveolar lumen fluid was obtained by flushing the lungs with EDTA-containing PBS (0,5 mM). Cell suspensions were stained with antibody cocktails in PBS for 30 min at 4°C, and subsequently washed in PBS before readout. Unspecific antibody binding was prevented by adding 2.4G2 (antibody to the Fcc receptor II/III) during the staining. A fixed amount of counting beads (123count ebeads, Thermo Fisher Scientific) was added to determine absolute cell numbers. Dead cells were excluded using the Fixable Viability Dye eFluor506 (eBioscience). Data acquisition was performed on a 4-laser Fortessa (BD Biosciences) and data were analyzed using FlowJo (Tree Star, Inc). Eosinophils were gated as CD11c- CD3/19- Ly6G- $CD11b^{hi}$, $SiglecF^{hi}$, $SSC\text{-}A^{hi}$; T-cells as CD11c- CD3/19+ MHCII- and B-cells as CD11c- CD3/19+ MHCII+.

FlowSOM

The automated analysis is done by the FlowSOM algorithm (1,2). FlowSOM uses a self-organizing map to cluster cells in different nodes based on the expression of the distinct

markers used in a given flow cytometry dataset and subsequently structures the nodes in a minimal spanning tree. We first concatenated live cells and used FlowSOM to generate a single FlowSOM tree.

Image quantification

To perform objective image quantification, a Fiji-based software script was applied to quantify PAS+ cells and α-SMA in the lung. To detect the whole tissue, RGB images were converted to 8-bit images and binary masks were created by the 'auto threshold mean' method (3). Filtering by size allowed to distinguish lung tissue from air space in the lung. Then, depending on the staining method, color deconvolution was applied as described in Ruifrok *et al*. (2001) (4). Positively stained cells were detected by the Renyi's Entropy thresholding method (5) and binary particle analysis was performed to filter particles by size. The positively stained area was then normalized to the total area of the lung.

Immunoblotting

Lung tissue was snap-frozen in liquid nitrogen during dissection. Lungs were homogenized with TissueLyser II (Qiagen) in 400µl E1A buffer (1% NP40, 20 mM HEPES, pH 7.9, 250 mM NaCl, 1 mM EDTA) complemented with cOmplete-ULTRA (Roche) protease inhibitors. Prior to SDS–PAGE, samples were spun at 12,000g to remove insoluble material. Protein concentration was determined by Bradford assay. Samples were boiled for 5 min at 95°C before loading. After wet transfer to polyvinyldifluoride membrane (Immobilon; Millipore), proteins were analyzed by immunoblotting and visualized by chemiluminescence (NEL 104001EA; Perkin Elmer). Primary antibodies used recognize beta-galactosidase (ab4761, Abcam, 1/1000) and beta-tubulin (ab21058, Abcam, 1/5000). Goat anti-rabbit-HRP (P0448, Dako, 1/2000) was used as secondary antibody.

1-DER T cell adoptive transfer

1-DER T cells were isolated out of spleen and lymph nodes from *Ormdl3*$^{wt/wt}$ and *Ormdl3*$^{Tg/wt}$ 1-DER mice. T cells were purified by making use of the MagniSort Mouse CD4 T cell Enrichment Kit (ThermoFisher) and were labeled with Cell Trace Violet (Invitrogen) during 10 minutes at 37°C. 1x10^6 1-DER cells of each genotype were intravenously injected into CD45.1 B6 acceptor mice, followed by intratracheal installation of 10 ug HDM 2 hours after IV injection. Acceptor mice were sacrificed 3 days later and mLN, lung and spleen were dissected for analysis.

Quantitative real time-PCR

Total RNA was isolated from mouse lung tissues by using the TriPure Isolation Reagent (Roche, Mannheim, Germany) and isolated according to the manufacturer's instructions. 1 ug RNA was converted to cDNA by an iScript advanced reverse transcriptase (Bio-Rad) according to manufacturer's instructions. The target cDNA was amplified by 30 cycles of PCR by using LightCycler® 480 Probes Master Mix (Roche) and the following primers: *Ormdl3*: (forward) CCCTCACCAACCTTATCCAC, (reverse) GGACCCCGTAGTCCATCTG; and universal probe #109 (Universal Probe Library, Roche, Indianapolis, IN, USA). Expression levels were calculated by using qBase+ software (Biogazelle, Ghent, Belgium) and normalized to the two most stable reference genes among *Hmbs*, *Sdha*, *Hprt*, *Rpl13a* and *Gapdh*. To amplify reference genes, SensiFAST SYBR® No-ROX Kit (GC Biotech) was used and primers were as follows: *Hmbs*: (forward) GAAACTCTGCTTCGCTGCATT, (reverse) TGCCCATCTTTCATCACTGTATG; *Sdha*: (forward) TTTCAGAGACGGCCATGATCT, (reverse) TGGGAATCCCACCCATGTT. *Hprt*: (forward) TGAAGAGCTACTGTAATGATCAGTCAAC, (reverse) AGCAAGCTTGCAACCTTAACCA; *Rpl13a* (forward) CCTGCTGCTCTCAAGGTTGTT,

(reverse) TGGTTGTCACTGCCTGGTACTT and *Gapdh*: (forward) GCATGGCCTTCCGTGTTC, (reverse) TGTCATCATACTTGGCAGGTTTCT.

Tissue homogenization preceding lipid extraction

Tissues were homogenized in lysis buffer [25 mM HEPES pH 8, 0.2% Triton X-100 (vol/vol)] using a Precellys 24 tissue homogenizer (Bertin Technologies, Montigny-le-Bretonneux, France). A volume that contained 100 mg protein (as determined by the Bradford assay) was filled up to 100 ml with saline for SL extraction.

Lipid extraction and sphingoid base analysis

Methanol (500 ml; Honeywell, Morris Plains, NJ, USA) containing 200 pmol internal standards (d7-sphinganine and d7-sphingosine; Avanti Polar Lipids, Alabaster, AL, USA) were added to tissue homogenate containing 100 mg protein, or 100 µl serum, followed by gentle rotation at 1400 rpm and 37°C for 1 h (Thermomixer comfort; Eppendorf, Hamburg, Germany). Samples were then centrifuged at 16,000 g for 5 min to pellet precipitated proteins, and supernatant was transferred to a new 2 ml Eppendorf tube. HCl (≥ 32%; Sigma-Aldrich) was added and lipids were hydrolyzed for 16 h at 65°C, then neutralized with 10 M KOH. Free sphingoid bases were extracted by adding chloroform (99.8%; Sigma-Aldrich) in basic conditions that contained 2N ammoniac (Sigma-Aldrich). Sphingoid bases were analyzed by using TSQ Quantum Ultra and Q Exactive liquid chromatography-mass spectrometry as previously described (6,7).

References

1. Van Gassen S, Callebaut B, Van Helden MJ, Lambrecht BN, Demeester P, Dhaene T, et al. FlowSOM: Using self-organizing maps for visualization and interpretation of cytometry data. Brinkman RR, Aghaeepour N, Finak G, Gottardo R, Mosmann T, Scheuermann RH, editors. Cytometry A. Wiley-Blackwell; 2015 Jul;87(7):636–45.

2. Guilliams M, Dutertre C-A, Scott CL, McGovern N, Sichien D, Chakarov S, et al. Unsupervised High-Dimensional Analysis Aligns Dendritic Cells across Tissues and Species. Immunity. 2016 Sep 20;45(3):669–84.

3. Glasbey C. An Analysis of Histogram-Based Thresholding Algorithms. Graphical Models and Image Processing. 1993 Nov;55(6):532–7.

4. Ruifrok AC, Johnston DA. Quantification of histochemical staining by color deconvolution. Anal Quant Cytol Histol. 2001 Aug;23(4):291–9.

5. Kapur JN, Sahoo PK, Wong AKC. A new method for gray-level picture thresholding using the entropy of the histogram. Computer Vision, Graphics, and Image Processing. 1985 Mar;29(3):273–85.

6. Othman A, Rütti MF, Ernst D, Saely CH, Rein P, Drexel H, et al. Plasma deoxysphingolipids: a novel class of biomarkers for the metabolic syndrome? Diabetologia. Springer-Verlag; 2012 Feb;55(2):421–31.

7. Ziv C, Malitsky S, Othman A, Ben-Dor S, Wei Y, Zheng S, et al. Viral serine palmitoyltransferase induces metabolic switch in sphingolipid biosynthesis and is required for infection of a marine alga. Proc Natl Acad Sci USA. 2016 Mar 29;113(13):E1907–16.

SUPPLEMENTARY FIGURE LEGENDS

Supplementary Figure 1: *Ormdl3*-LacZ reportermice as a useful tool to study ORMDL3 expression

A) Western blot showing β-galactosidase expression in different tissues from an *Ormdl3*-LacZ reporter mouse. For each tissue, 50 ug of protein (determined by Bradford assay) was loaded. β-tubulin was used as a loading control.

B) Heat map showing *Ormdl3* mRNA expression in different murine tissues. The heatmap demonstrates publicly available RNA-seq data from the Genevestigator database.

C) Western blot showing β-galactosidase expression in lung tissue from PBS-sensitized (non-asthmatic) mice and HDM-sensitized (asthmatic) *Ormdl3*-LacZ reporter mice. β-tubulin was used as a loading control.

Supplementary Figure 2: Effect of altered ORMDL3 expression on sphingolipid concentration

A) Schematic overview of sphingolipid synthesis. *De novo* sphingolipid synthesis starts with the action of serine palmitoyl transferase (SPT), which mediates the condensation of serine

and palmitoyl-CoA into long-chain bases such as sphinganine. Sphinganines are subsequently acylated to form (dihydro)ceramides by the action of ceramide synthases (CERS). In the Golgi, ceramides can be converted to more complex sphingolipids such as sphingomyelin, or can be broken down by ceramidases to form sphingosine. Sphingosine-1-phosphate (S1P), the phosphorylated form of sphingosine, is the substrate of S1P-lysase (SGPL), which is the only enzyme converting sphingolipids into non-sphingolipid molecules. KDSR = 3-ketodihydrosphingosine reductase; DEGS = sphingolipid delta(4)-desaturase; SPHK = sphingosine kinase; SA1P = sphinganine-1-phosphate; SGPP = sphingosine-1-phosphate phosphatase 1.

B-P) Ceramide, hexosylceramide, and sphingomyelin levels in different tissues from (non)-asthmatic *Ormdl3*$^{wt/wt}$ and *Ormdl3*$^{Tg/wt}$ mice (upper part) and *Ormdl3*$^{+/+}$ and *Ormdl3*$^{-/-}$ mice (lower part). B-D: lung; E-G: serum; H-J: liver; K-M: brown adipose tissue (BAT); N-P: white adipose tissue (WAT).

Data information: All data were analyzed with a Shapiro-Wilk normality test to assess whether the data was normally distributed. Parametric data were analyzed with an ordinary one-way ANOVA test with multiple comparison correction. Non-parametric data were analyzed with an unpaired Kruskal-Wallis test with multiple correction. Data are shown as means +/- SEM. *p<0.05; **p<0.01, ***p<0.001; ****<0.0001. Upper panels (*Ormdl3*$^{wt/wt}$ and *Ormdl3*$^{Tg/wt}$ mice): n=8,13,6,10; lower panels (*Ormdl3*$^{+/+}$ and *Ormdl3*$^{-/-}$ mice): n=5,5,7,7.

Supplementary Figure 3: ORMDL3 overexpression does not affect allergic asthma driven by acute or chronic HDM exposures

A) Number of inflammatory cells in bronchoalveolar lavage (BAL) fluid from mock- and HDM-sensitized *Ormdl3*$^{wt/wt}$ and *Ormdl3*$^{Tg/wt}$ mice (n=5,11,7,15).

B) Protein levels of IL-10 and IL-17A secreted by mediastinal lymph node cells during restimulation with HDM for three days (n=5,11,7,15).

A/B) Data were pooled from 2 independent experiments.

C) Scheme representing the chronic HDM-dependent asthma model.

D) *Ormdl* mRNA expression levels in lung tissue from PBS and HDM-treated *Ormdl3*$^{wt/wt}$ and *Ormdl3*$^{Tg/wt}$ mice. Expression values were calculated by using qBase+ and were normalized to reference genes *Hmbs* and *Hprt*. Expression values are shown relative to means of the PBS-treated *Ormdl3*$^{wt/wt}$ group (n=5,8,5,7).

E) Number of inflammatory cells in BAL fluid from PBS and HDM-treated *Ormdl3*$^{wt/wt}$ and *Ormdl3*$^{Tg/wt}$ mice (n=5,8,5,8).

F) Protein levels of IL-5 and IL-13 secreted by mediastinal lymph node cells during restimulation with HDM for three days (n=5,8,5,8).

G) Serum HDM-specific immunoglobulin G1 (IgG1) and HDM-IgE as measured by ELISA (n=5,8,5,8).

Data information: All data were analyzed with a Shapiro-Wilk normality test to assess whether the data was normally distributed. Parametric data were analyzed with an ordinary one-way ANOVA test with multiple comparison correction. Non-parametric data were analyzed with an unpaired Kruskal-Wallis test with multiple correction. Data are shown as means +/- SEM. *p<0.05; **p<0.01, ***p<0.001; ****<0.0001.

Supplementary Figure 4: ORMDL3 does not affect T cell function intrinsically

A) Scheme representing the adoptive transfer of *Ormdl3*$^{wt/wt}$ and *Ormdl3*$^{Tg/wt}$ 1-DER T cells into CD45.1 B6 acceptor mice, which were consequently exposed to HDM.

B) Proliferation profile of adoptively transferred 1-DER T cells labelled with CTV 3 days after transfer.

C) Proliferation and number of adoptively transferred 1-DER T cells 3 days after transfer (n=7,7).

Supplementary Figure 5: ORMDL3 overexpression does not affect allergic asthma driven by *Alternaria alternata*

A) Scheme representing the *A. alternata*-dependent asthma model.

B) *Ormdl* mRNA expression levels in lung tissue from *Ormdl3*$^{wt/wt}$ and *Ormdl3*$^{Tg/wt}$ mice exposed to either PBS or *A. alternata*. Expression values were calculated by using qBase+ and were normalized to reference genes *Hprt* and *Sdha*. Expression values are shown relative to means of the PBS-treated *Ormdl*3$^{wt/wt}$ group (n=1,7,1,4).

C) Western blot showing β-galactosidase expression in lung tissue from non-asthmatic (PBS-treated) and asthmatic (*A. alternata*-treated) *Ormdl3*-LacZ reportermice. β-tubulin was used as a loading control.

D) Number of B and T lymphocytes in BAL fluid from *Ormdl3*$^{wt/wt}$ and *Ormdl3*$^{Tg/wt}$ mice treated with PBS or *A. alternata* (n=3,24,3,22).

E) Serum *A. alternata*-specific IgG1 (OD value) as measured by ELISA (n=1,8,1,9).

F) Protein levels of IL-5, IL-13 and IL-10 secreted by mediastinal lymph node cells during restimulation with *A. alternata* for three days (n=3,24,3,22).

D/F) Data were pooled from 3 independent experiments.

Data information: All data were analyzed with a Shapiro-Wilk normality test to assess whether the data was normally distributed. Parametric data were analyzed with an ordinary one-way ANOVA test with multiple comparison correction. Non-parametric data were analyzed with an unpaired Kruskal-Wallis test with multiple correction. Data are shown as means +/- SEM. *p<0.05; **p<0.01, ***p<0.001; ****<0.0001.

Supplementary Figure 6: Loss of *Ormdl3* expression does not affect allergic asthma driven by HDM or *Alternaria alternata*

A) Number of inflammatory cells in BAL fluid from mock- and HDM-sensitized *Ormdl3*$^{+/+}$ and *Ormdl3*$^{-/-}$ mice (n=10,11,7,14).

B) Number of neutrophils in BAL fluid and protein levels of IL-17A secreted by mediastinal lymph node cells during restimulation with HDM for three days (n=10,11,7,14).

C) *Ormdl* mRNA expression levels in lung tissue from *Ormdl3*$^{+/+}$ and *Ormdl3*$^{-/-}$ mice exposed to either PBS or *A. alternata*. Expression values were calculated by using qBase+ and were normalized to reference genes *Hprt* and *Rpl13a*. Expression values are shown relative to means of the PBS-treated Ormdl3$^{+/+}$ group (n=4,5,4,6).

D) Number of B and T lymphocytes in BAL fluid from *Ormdl3*$^{+/+}$ and *Ormdl3*$^{-/-}$ mice treated with PBS or *A. alternata* (n=6,23,2,22). Data were pooled from 3 independent experiments.

E) Protein levels of IL-5, IL-13 and IL-10 secreted by mediastinal lymph node cells during restimulation with *A. alternata* for three days (n=4,14,4,13).

F) Serum *A. alternata*-specific IgG1 (OD value) as measured by ELISA (n=4,6,4,6).

A/B/E) Data were pooled from 2 independent experiments.

Data information: All data were analyzed with a Shapiro-Wilk normality test to assess whether the data was normally distributed. Parametric data were analyzed with an ordinary one-way ANOVA test with multiple comparison correction. Non-parametric data were analyzed with an unpaired Kruskal-Wallis test with multiple correction. Data are shown as means +/- SEM. *p<0.05; **p<0.01, ***p<0.001; ****<0.0001.

Figure No.1

Click here to access/download;Figure No.;Figure1.pdf

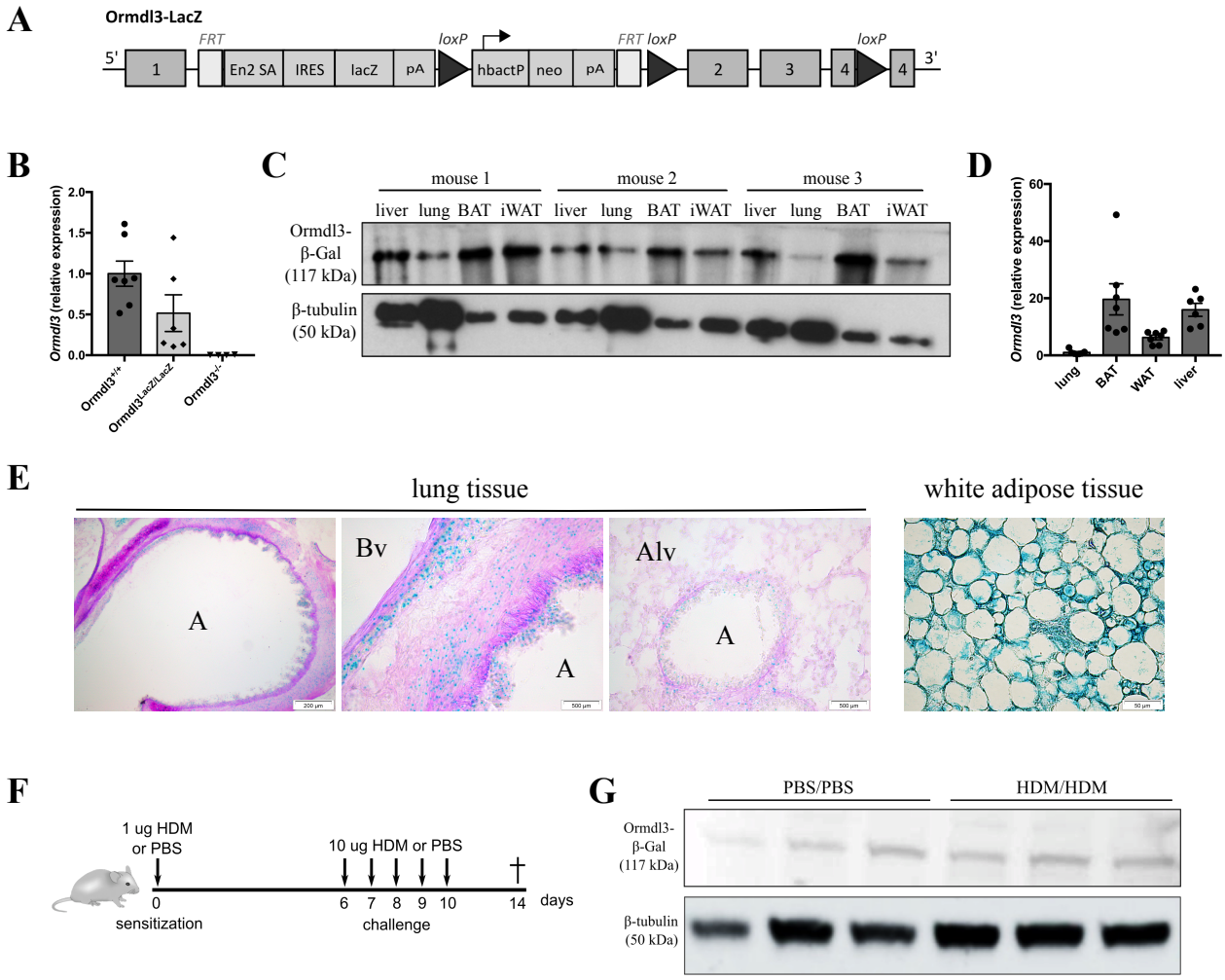

Figure No.2

Click here to access/download;Figure No.;Figure2.pdf

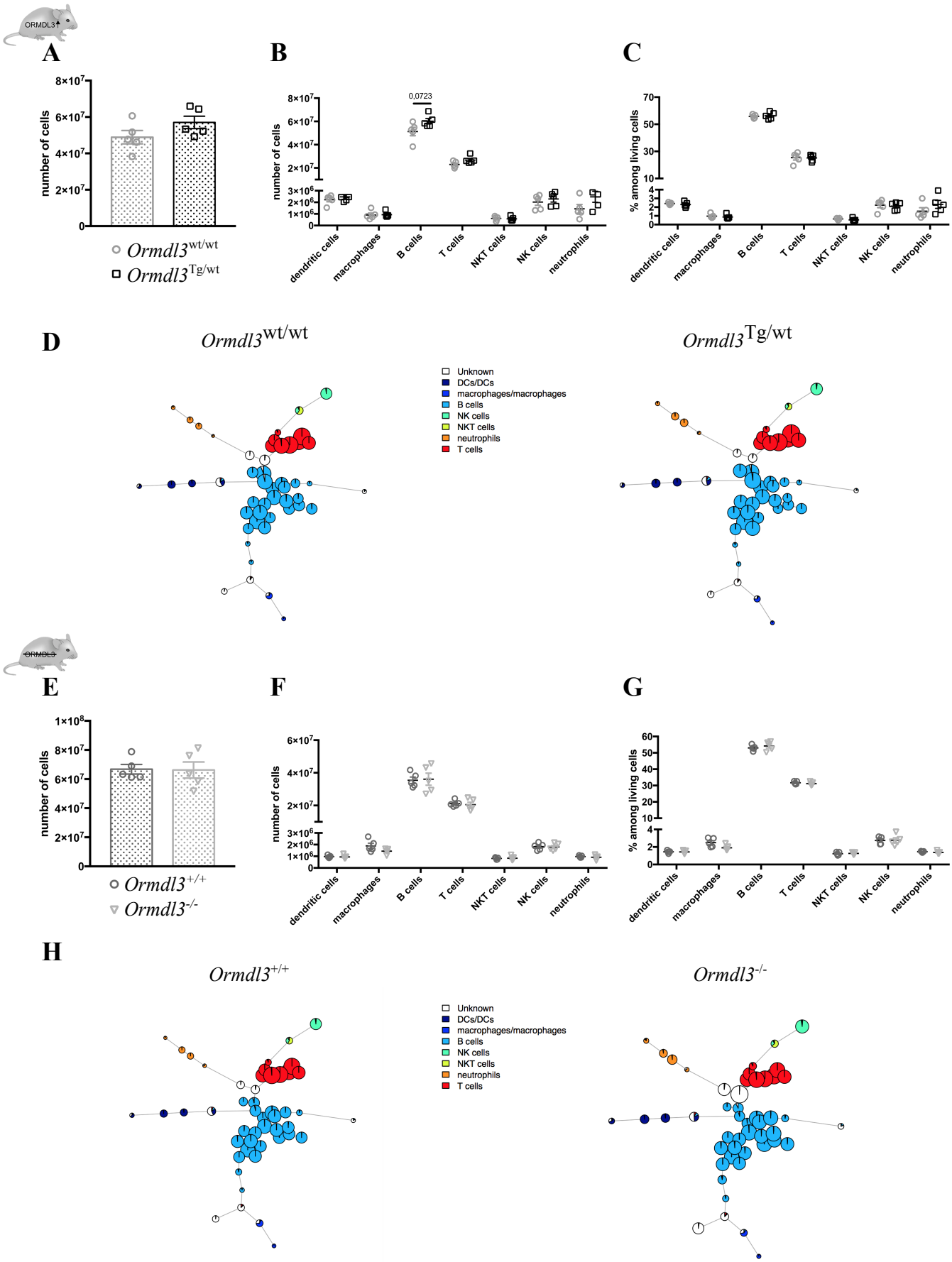

Figure No.3

Click here to access/download;Figure No.;Figure3.pdf

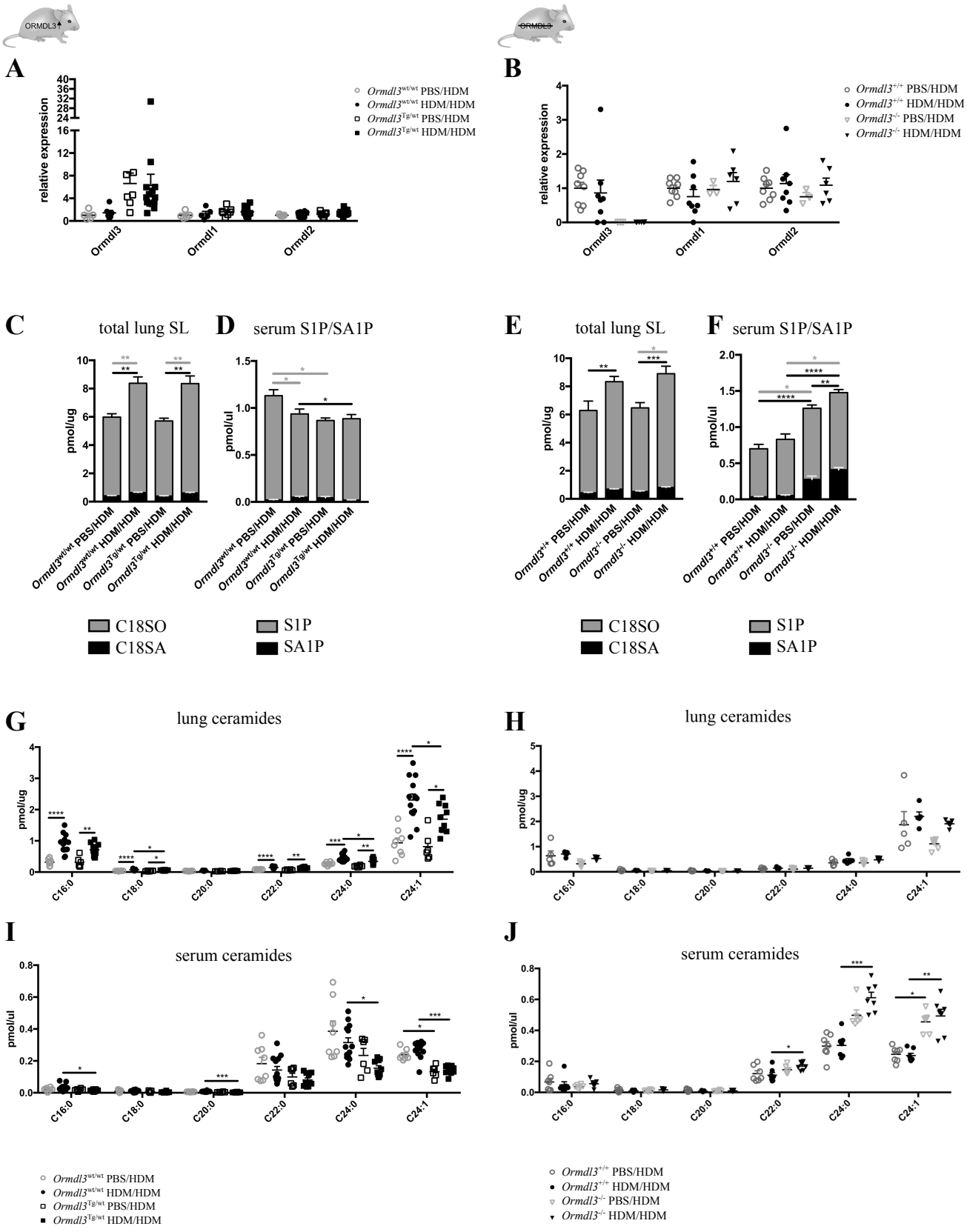

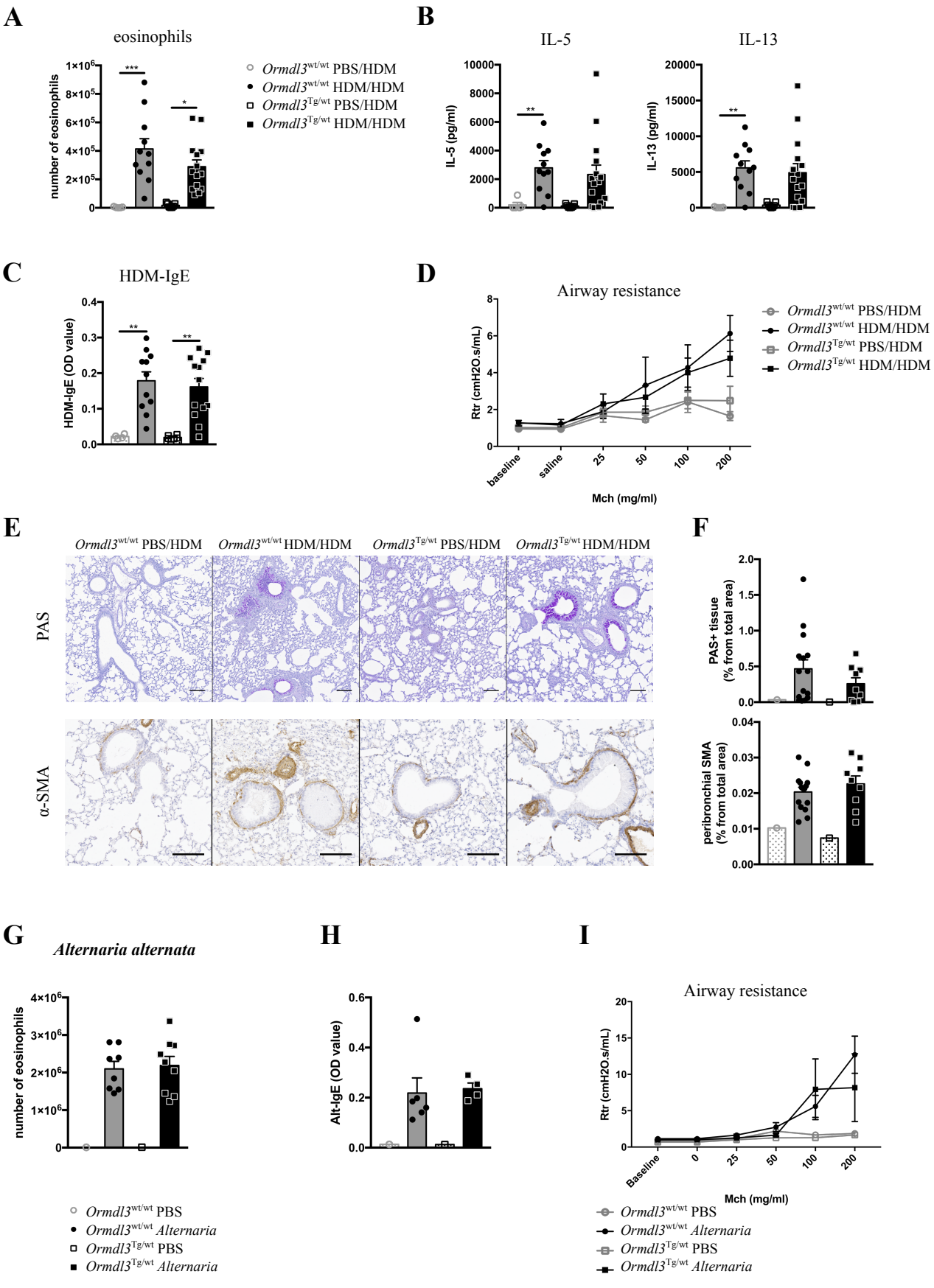

Figure No.5

Click here to access/download;Figure No.;Figure5.pdf

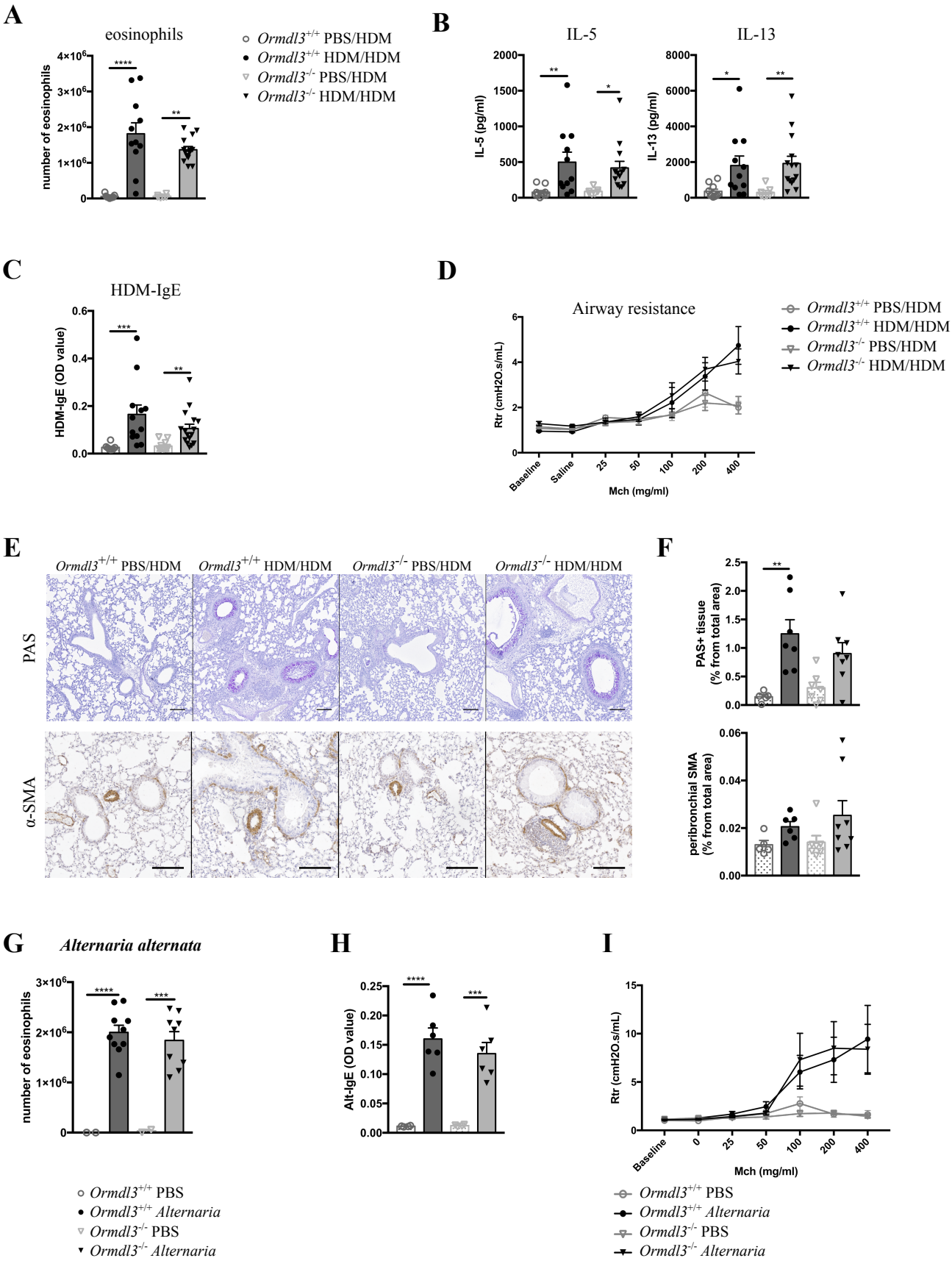

A

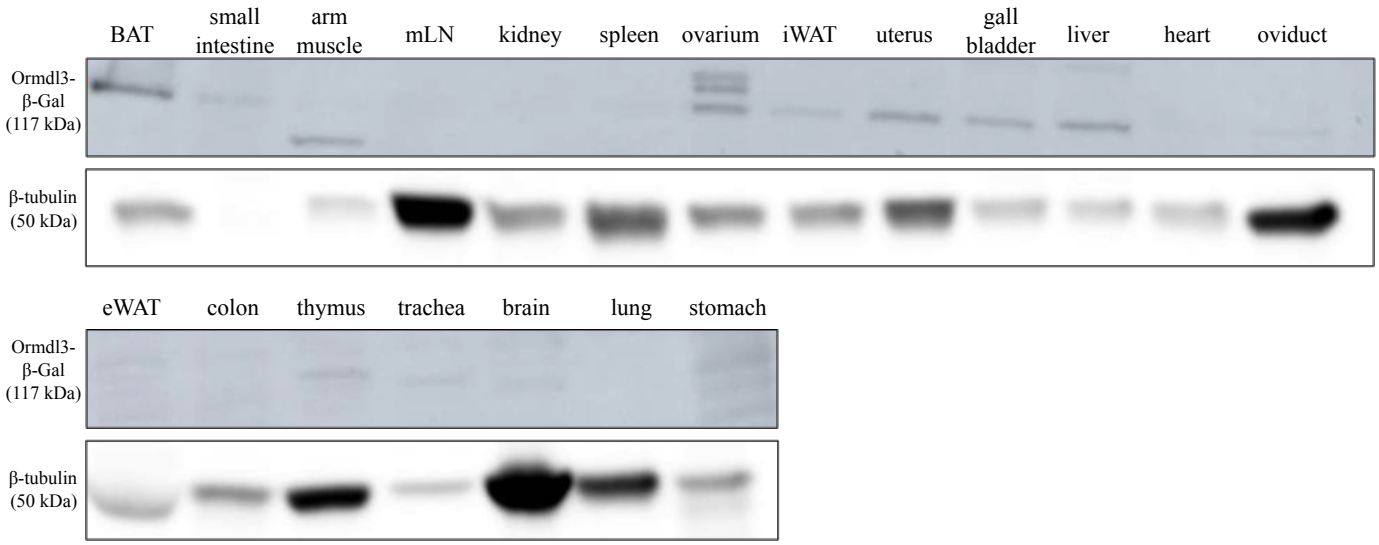

B

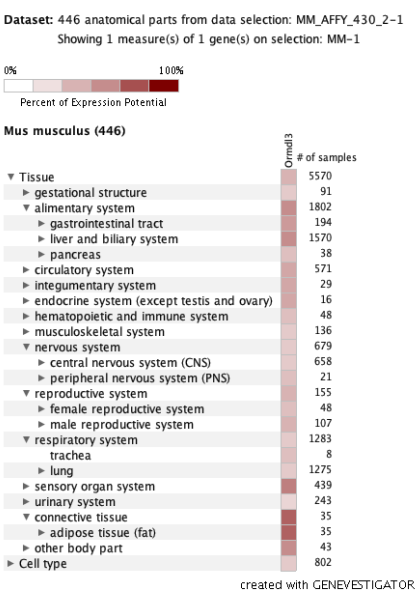

C

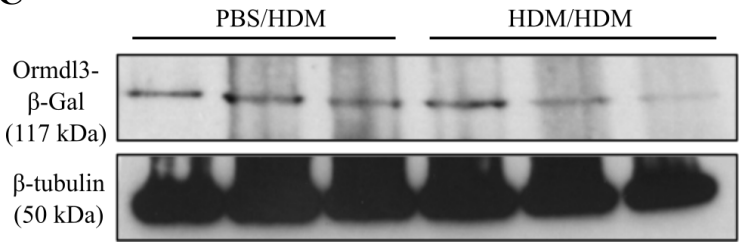

Suppl Figure No.2A

Click here to access/download;Figure No.;Suppl. Fig2.pdf

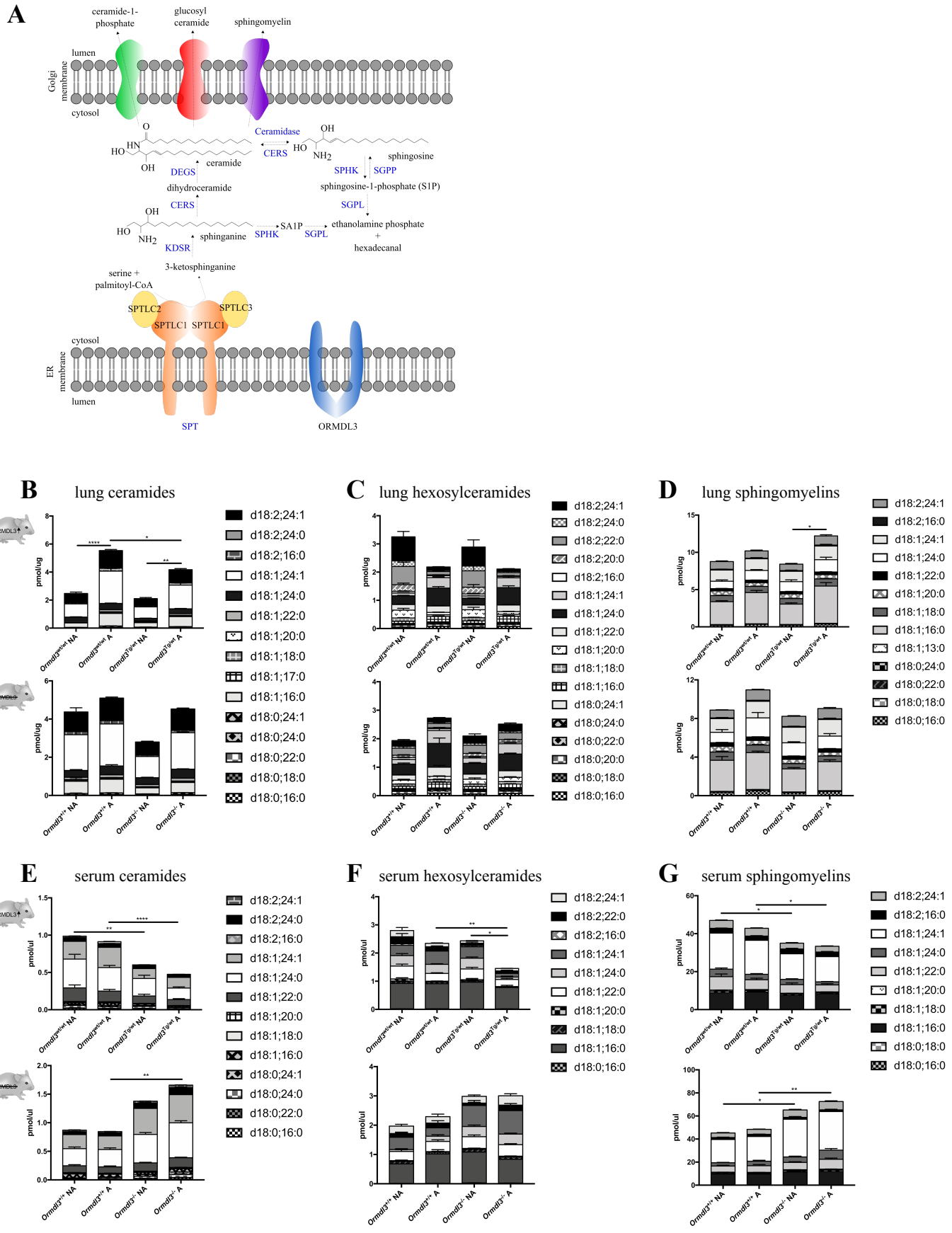

Suppl Figure No.2B

Click here to access/download;Figure No.;Suppl. Fig2 vervolg.pdf